

CORRELATION BETWEEN AGING TIME PERIOD OF METAL PRECURSOR SOL – PHASE COMPOSITION AND TEXTURAL PROPERTIES OF ZIRCONIA NANOPOWDERS

Eva Mitkova¹, Irina Stambolova²,
Daniela Stoyanova², Vesislava Toteva¹, Ognian Dimitrov³

¹University of Chemical Technology and Metallurgy
8 Kliment Ohridski Blvd., Sofia 1797, Bulgaria

²Bulgarian Academy of Sciences
Institute of General and Inorganic Chemistry
Acad. G. Bonchev str., bl. 11, Sofia 1113, Bulgaria

³Bulgarian Academy of Sciences
Institute of Electrochemistry and Energy Systems
Acad. G. Bonchev str., bl. 10, Sofia 1113, Bulgaria
Email: vesislava@uctm.edu

Received 05 June 2023

Accepted 21 July 2023

DOI: 10.59957/jctm.v59.i1.2024.26

ABSTRACT

This article investigates the effect of the time of aging of ZrO₂ powders, obtained from zirconium butoxide sols, stabilized using complexing agents on the volume phase fractions tetragonal phase (T) and baddeleyite crystallographic phase (B), pore size distribution and pore volume. It was proved that the aging time period influences ratio between these two polymorphs of zirconia. The sample Zr3d possesses the largest content of baddeleyite phase having the greatest crystallites in comparison to another two powders. The increasing of aging period leads to a gradual increase in (101) peak intensity of T phase, while all the samples are microporous regardless of the aging time. The longest time aged sample possesses higher pore volume and higher average pore diameter than the other two powders. The physico-chemical features of the prepared ZrO₂ nanosized powders could be beneficial as catalysts/ photocatalysts in different catalytic reactions, corrosion inhibition particles, etc.

Keywords: sol - gel, morphology, phase composition, phase transformation, zirconia nanoparticles.

INTRODUCTION

Zirconium dioxide (ZrO₂) is material having excellent physico-chemical properties: good thermal stability, high strength, abrasion/corrosion and chemical resistance, antibacterial properties and ionic conductivity. These properties make it suitable for a variety of industrial and medical applications [1, 2]. Zirconium oxide ceramics have often been chosen for joining ceramic and steel, due to its remarkably high thermal expansion. Zirconium oxide is well known to be a highly active catalyst and its activity is higher than those of strongly acidic or basic catalysts [3, 4]. It is also applied as a catalyst support [5], oxygen sensor [6], NO₂ sensor [7], photocatalyst for degradation of dyes

[8], antimicrobial material in industry [9], implants in dental medicine [10], optical lenses [11], etc.

Sol - gel is one of the most often applied, low-cost, and flexible method to produce thin films and powders. The main advantages of the sol-gel process are the narrow particle size distribution, uniform nanostructure at low temperatures and possibility to produce high quality for two or more types of nanoparticles simultaneously on industrial scale [12]. Roy and co-workers in the 1950s and 1960s have synthesized a large number of novel ceramic oxide compositions on the basis of Al, Si, Ti, Zr, etc., achieving very high levels of chemical homogeneity in colloidal gels [13 - 15]. Lately, the controlled hydrolysis of alkoxides has been used to produce submicrometer size TiO₂ [16],

ZrO₂ and SiO₂ [18] powders. In sol - gel process, the following basic physico-chemical steps proceed: aging, drying, stabilization and densification. During the aging stage, polycondensation, syneresis, coarsening and phase transformation can occur. As a result of aging, the structure and properties of the gel are considerably changed. It is possible to control the porosity by varying of the drying conditions of the gel. The connectivity of the network increases due to the polycondensation reactions, which involves the establishment of M-OH-M or M-O-M (where M represents the metal atom) between the metal atoms in the raw materials. Syneresis step leads to expulsion of liquid from the pores. After this step, the surface area decreases through dissolution and reprecipitation processes (coarsening step). Among the other technological parameters of the sol - gel process, the aging time interval has critical effect on the microstructure and on the phase composition of the sol - gel powders (e.g. oxides). During aging, polycondensation continues, which increases the thickness of interparticle necks as a result the porosity decreases and the gel strength increases.

This article presents the results of the investigated effect of the time period of aging of alcohol-based sols (using zirconium butoxide and acetyl acetone and acetic acid as complexing agents) on the phase evolution and texture of the ZrO₂ powders, aiming at various applications: as catalysts in different chemical reactions, corrosion inhibition particles, etc.

EXPERIMENTAL

Preparation of zirconia samples

The precursor solution was prepared using Zr(OBu)₄, dissolved in 20 mL of isopropyl alcohol. This mixture was added dropwise to a mixture of 8.6 mL acetyl acetone (AcAc), 5.6 mL acetic acid and isopropanol under continuous stirring for 1 h (solution A). Then small amounts of polyethylene glycol (PEG400) and HNO₃ were added to the solution A. The final solution B is diluted adding isopropanol to 0.2 M. Thus, prepared final solution was divided in 3 parts. An aging procedure was conducted at room temperature (25°C) with different durations: 1 day, 3 days and 180 days. The dried powders are thermally treated in a programmable oven at 500°C for 3 hours in air. Thus obtained ZrO₂ powders was signed as: Zr-1d, Zr-3d, Zr-180d.

Characterization

The phase compositions of the samples were investigated by means of X-ray diffraction (XRD) using a Bruker D2 Phaser diffractometer, Karlsruhe, Germany (Cu K radiation at 40 kV). An automated apparatus NOVWin-CFR Quantachrom-Gas Sorption System, Florida, USA was applied to estimate the pore size distribution (DFT method). The infrared spectra (4000 cm⁻¹ - 400 cm⁻¹ region) were registered using a Thermo Scientific Nicolet iS5 Fourier-transform IR spectrometer (KBr pellets, resolution of 2 cm⁻¹). Scanning electron microscopy (SEM) micrographs were recorded on a JEOL JEM-200CX at an accelerating voltage of 80 keV. EDX analyses were carried out on four different points and revealed similar chemical composition. The differential thermal analysis was accomplished on a combined DTA-TG apparatus LAB-SYSEVO 1600, manufactured by the SETARAM Company (Caluire, France) using synthetic air (flow rate of 20 mL·min⁻¹); heating rate 10°C/min; temperature interval ranging from 25°C to 800°C. A corundum crucible and a Pt/Pt-Rh thermocouple were used.

RESULTS AND DISCUSSION

X-ray phase analysis revealed that the obtained ZrO₂ powders contain tetragonal phase (T) and baddeleyite (B) crystallographic phase (Fig. 1, Table 1). A gradual increasing in (101) peak intensity of tetragonal phase was observed. This could be due to the recrystallization process and aging of the obtained material. Shevchenko et al. have studied the effect of aging on ceria doped ZrO₂ gels [19]. They have proved that the increasing of the aging time interval increases the structural

Table 1. Phase composition and crystallites sizes of the ZrO₂ samples.

Sample	Tetragonal phase (98-009-7004), content, % Size of the crystallites, nm	Baddeleyite (98-006-0900), content, % Size of the crystallites, nm
Zr1d	90.8 / 10	9.2 / 12
Zr3d	88 / 8	12 / 14
Zr180d	97.2 / 10	2.8 / 5

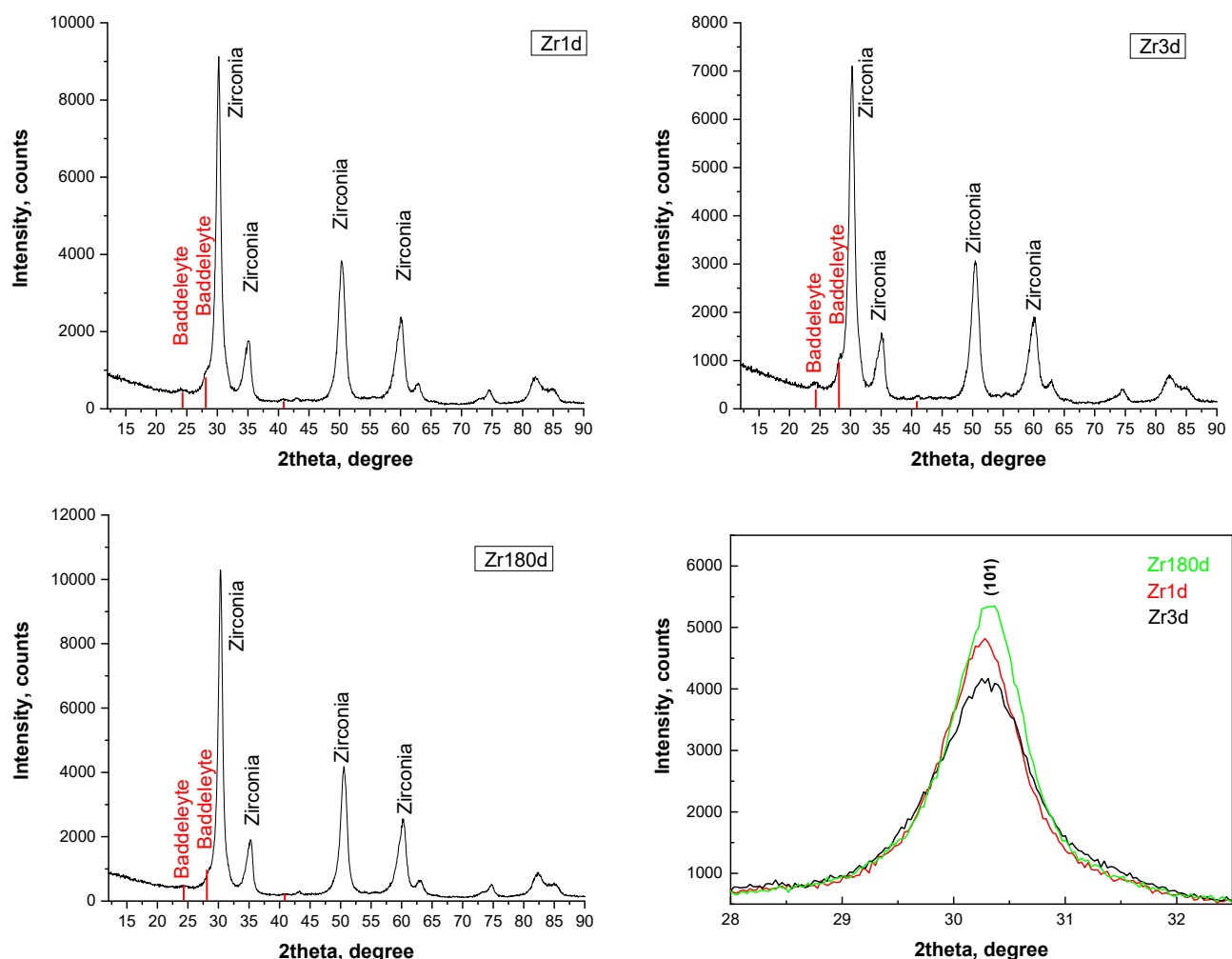


Fig. 1. X-ray diffractograms of ZrO_2 samples, aged for different time and the (101) peak intensity of the tetragonal phase.

perfection, but it has little influence on the crystallites size. Table 1 revealed that the sample Zr3d possesses the largest content of baddeleyite phase with the greatest crystallites, while for the other two powders the tetragonal phase possesses the smallest crystallites.

In order to determine the appropriate heat treatment regime of the samples, DTA/TG analysis of the precursor solution dried at 100°C (Fig. 2) was applied. Small endothermic peak at 100°C , which corresponds to the loss of adsorbed water was recorded. The registered four small exothermic peaks in the DTA curve could be due to the gradual decomposition of a larger amount of organic residues. The exothermic peak at 535°C corresponds to the crystallization of ZrO_2 tetragonal and baddeleyite phases from the amorphous material. According to some other researchers the transformation

tetragonal (T) to monoclinic baddeleyite (B) phase is registered at higher temperature - 600°C , which is due to the stabilizing role of complexating agent acetic acid [20]. In our case, probably the presence of zirconium butoxide, AcAc (complexating agent) and nitric acid (catalyst) promote the transformation T to B phase at lower temperature.

Randomly oriented plate-like particles are visible on the SEM photographs of the sample Zr1d, Fig 3(a). After 3 and 180 days aging time period, the shape of the particles are not significantly changed (Fig. 3(b), (c)). After thermal treatment at 500°C one observes the same type of morphology but having more compact type. In the case of sample Zr180d an enlargement of the plates is observed. The chemical composition of the powders, evaluated by EDX analyses are similar, (Fig. 4).

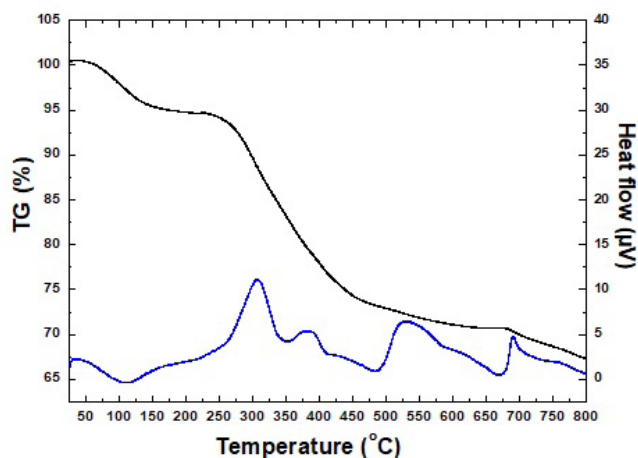


Fig. 2. DTA of the powder, obtained after drying at 100°C (TG- black line, heat flow- blue line).

The physicochemical changes due to the hydrolysis-condensation processes, as well as the phase transformations in the gels were determined by infrared spectroscopy, Fig. 5(a). The absorption broad bands in the region 3000 cm^{-1} - 3600 cm^{-1} corresponds to the vibrational frequencies of OH groups, due to adsorbed water molecules and surface H-bonding hydroxyl groups. The spectrum exhibits the bands corresponding to the stretching and bending vibrations of the CH_3 and CH_2 groups, within the ranges of 2980 cm^{-1} - 2870 cm^{-1} and 1460 cm^{-1} - 1380 cm^{-1} , respectively. Within the region 1550 cm^{-1} - 1400 cm^{-1} are registered peaks corresponding to carbonate and hydrogen carbonate groups. The band at 785 cm^{-1} and the bands in the 1050 cm^{-1} - 1150 cm^{-1} region correspond to vibrations of the CH groups of the organic precursors (butoxy group belonging to zirconium butoxide) [21]. The band at 780 cm^{-1} , which is due to the $\nu(\text{Zr-Obr})$ stretching vibration [21]. The bands at 616 cm^{-1} and 655 cm^{-1} correspond to Zr-O and Zr-O-Zr vibrations.

All the peaks corresponding to organic groups were not observed in the infrared spectra of the thermally treated precursors (aging time: 3 and 180 days), Fig. 5(b). The bands corresponding to Zr-O and Zr-O-Zr vibrations were observed. The inset picture on Fig. 5(b) represents peaks, which belong to carbonate and hydrogen carbonate groups, while the peak at 1634 cm^{-1} corresponds to the vibrational frequencies of OH groups.

The adsorption - desorption isotherms of the powders are shown in Fig. 6(a). A difference in the hysteresis sections of the two samples is observed. In

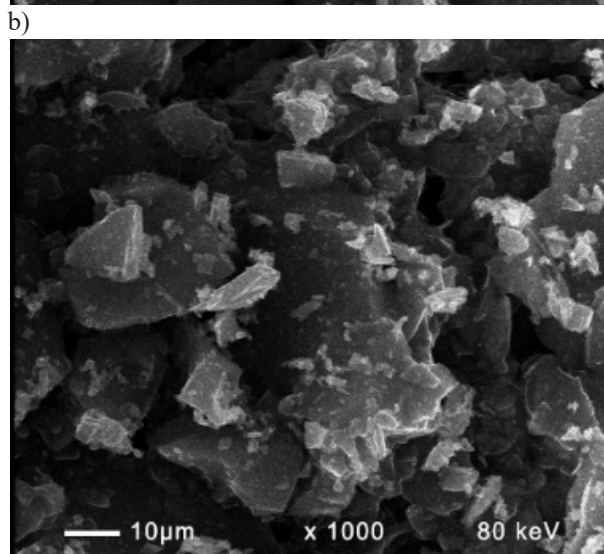
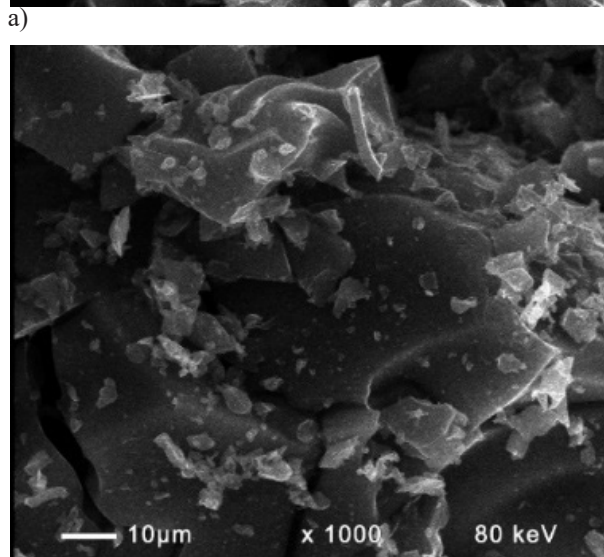
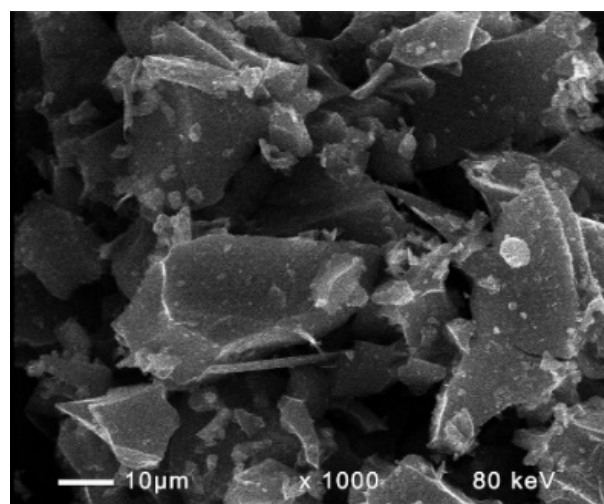


Fig. 3. SEM photograph of sol aged precursor powder Zr1d (a), Zr3d (b) and Zr180d (c) dried at 100°C at 10 µm magnifications, respectively.

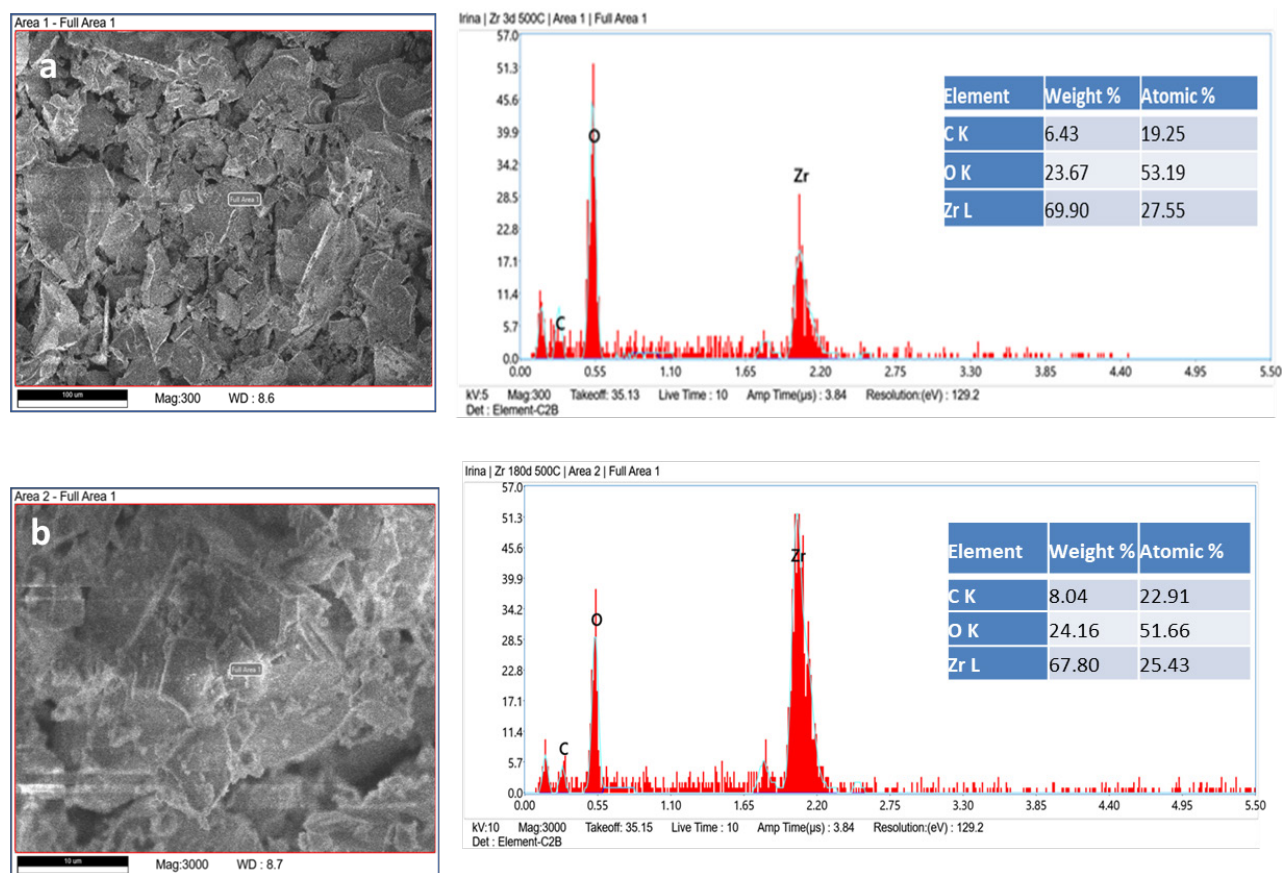


Fig 4. SEM photographs and EDX spectra of powder Zr3d (a) and Zr180d (b), treated at 500°C.

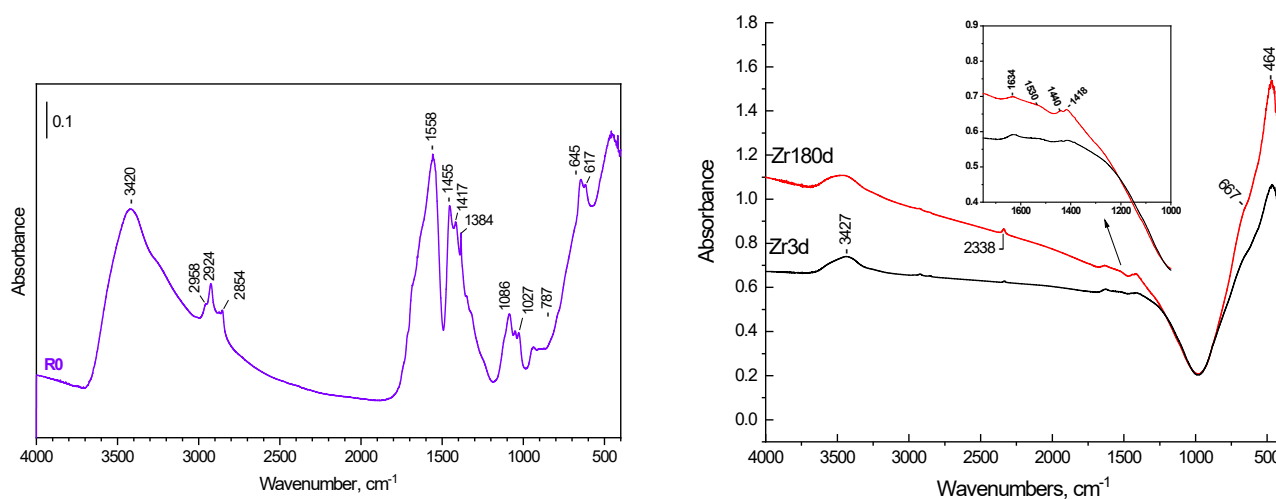


Fig. 5. IR spectrum a) - of the precursor Zr3d dried at 100°C; b) - of the precursors Zr3d and Zr180d, thermally treated at 500°C.

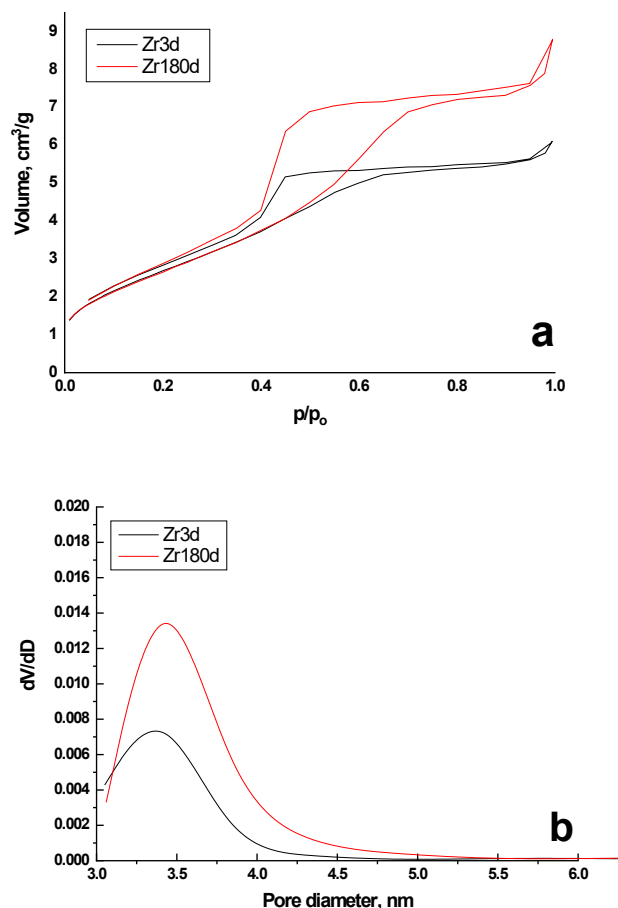


Fig. 6. BET surface area (a) and pore size distribution (b) of sol-aged precursors.

Table 2. Specific surface area (S), pore volume (V_t) and average pore sizes (D_{av}) of the samples

Sample	S, m ² /g	V _t , cm ³ /g	D _{av} , nm
Zr3d	10	0.009	3.7
Zr180d	10	0.014	5.3

accordance with the UPAC nomenclature the sample Zr3d shows a hysteresis section, which is closer to type H4. The sample Zr180d has modified type of isotherm H4. These facts are indications for the presence of micropores in the structure. The samples do not reveal any substantial difference in the pore size distribution, Fig. 6(b).

The powders exhibit only one broad peak appearing in the pore size region varying from 3 to 5 nm, which corresponds to micropores. The specific surface areas

of the samples are the same (Table 2). The sample, aged longer time period (180 days) possesses higher pore volume and higher average pore diameter than the other powder.

CONCLUSIONS

Nanosized mixed phase ZrO₂ powders have been prepared using zirconium butoxide precursor sols, aged for 1, 3 and 180 days and treated at 500°C. The time of aging of zirconia sols has effects on the following parameters: volume phase fractions T : B, pore size distribution and pore volume. It was registered that there two polymorphs of ZrO₂ in all samples: tetragonal and baddeleyite with various volume fractions present. The sample Zr3d possesses the largest content of baddeleyite phase with the greatest crystallites in comparison to the other two powders. A gradual increasing in (101) peak

intensity of tetragonal phase was proved upon increasing of aging period of time. The morphology and chemical composition of all powders are similar. The samples are microporous regardless of the aging time. The longest time aged sample possesses higher pore volume and higher average pore diameter than other two powders. The simultaneous presence of mixed ZrO₂ phases as well the presence of micropores could be beneficial for the catalytic/photocatalytic activity, due to close contact between the particles of each constituent phase.

Acknowledgements

The authors are grateful to the financial support by project No.KP-06-N37/16 „New environmentally friendly one- and multi-layer coatings for corrosion protection of structural materials with wide application” of Bulgarian National Science Fund at the Ministry of Education and Science of Bulgaria, as well as the contract „Environmentally friendly anticorrosive hybrid coatings “within the non-currency Equivalent Exchange Bilateral Cooperation between the Bulgarian Academy of Sciences and the Serbian Academy of Sciences and Fine Arts.

REFERENCES

1. D. Stoyanova, I. Stambolova, M. Shipochka, N. Boshkova, S. Simeonova, N. Grozev, G. Avdeev, O. Dimirov, N. Boshkov, Protective Efficiency of ZrO₂/Chitosan “Sandwich” Coatings on Galvanized Low-Carbon Steel, MDPI, Coatings, 11, 9, 2021, 1103.
2. P.Fr. Manicone, P.R. Iommetti, L. Raffaelli, An overview of zirconia ceramics: Basic properties and clinical applications, J. Dent., 35, 2007, 819-826.
3. I. Atribak, N. Guillén-Hurtado, A. Bueno-López, A. García-García, Influence of the physico-chemical properties of CeO₂-ZrO₂ mixed oxides on the catalytic oxidation of NO to NO₂, Appl. Surf. Sci., 256, 2010, 7706-7712.
4. E. Hong, C. Kim, D.-H. Lim, H.-J. Cho, C.-H. Shin, Catalytic methane combustion over Pd/ZrO₂ catalysts: Effects of crystalline structure and textural properties, Appl. Catal. B, 232, 2018, 544-552.
5. C.-M. Zhi, R.-H. Yang, C.-Y. Zhou, G.-R. Wang, J.-Y. Ding, W. Yang, Unraveling the role of Ni₁₃ catalyst supported on ZrO₂ for CH₄ dehydrogenation: The d-band electron reservoir, J. Fuel Chem. Technol., 50, 2022, 601-609.
6. T. Wen, L. Yuan, Z. Yan, Y. Jin, Z. Liu, J. Yu, Enhancement of the electrochemical performance in MgO stabilized ZrO₂ oxygen sensors by co-doping trivalent metal oxides, Curr. Appl. Phys., 39, 2022, 133-139.
7. Y. Yan, Z. Ma, J. Sun, M. Bu, Y. Huo, Z. Wang, Y. Li, N. Hu, Surface microstructure-controlled ZrO₂ for highly sensitive room-temperature NO₂ sensors, Nano Mater. Sci., 3, 2021, 268-275.
8. S.P. Keerthana, R. Yuvakkuma, P.S. Kumar, G. Ravi, D. Velauthapillai, Nd doped ZrO photocatalyst for organic pollutants degradation in wastewater, Environ. Technol. & Innov., 28, 2022, 102851.
9. J.B. Fathim, A. Pugazhendhi, R. Venis, Synthesis and characterization of ZrO₂ nanoparticles-antimicrobial activity and their prospective role in dental care, Micr. Pathogen, 110, 2017, 245-251.
10. G.I. Benic, D.S. Thoma, I. Sanz-Martin, F. Munoz, C.H.F. Hämmerle, A. Cantalapiedra, J. Fischer, R.E. Jung, Guided bone regeneration at zirconia and titanium dental implants: a pilot histological investigation, Clinin. Oral Implants Res., 28, 2017, 1592-1599.
11. U. Peuchert, Y. Okano, Y. Menke, S. Reichel, A. Ikesue, Transparent cubic-ZrO₂ ceramics for application as optical lenses, J. Europ. Ceram. Soc. 29, 2009, 283-291.
12. R. Xu, D. Wang, J. Zhang, Y. Li, Shape-dependent catalytic activity of silver nanoparticles for the oxidation of styrene, Chemistry - An Asian Journal, 1, no. 6, 2006, 888-893.
13. D.M. Roy, R. Roy, Experimental study of the formation and properties of synthetic serpentines and related layer silicate minerals, American Mineralogist, 39, 1954, 957-975.
14. R. Roy, Aids in Hydrothermal Experimentation: II, Methods of Making Mixtures for Both “Dry” and “Wet” Phase Equilibrium Studies, J. Amer. Ceram. Soc, 39, 1956, 145-146.
15. R. Roy, Gel Route to Homogeneous Glass Preparation, J. Amer. Ceram. Soc., 52, 1969, 344-344.
16. E.A. Barringer, H.K. Bowen, Formation, Packing, and Sintering of Monodisperse TiO₂ Powders, J. Amer. Ceram. Soc., 65, 1982, C199-C201.
17. B. Fegley Jr., P. White, H.K. Bowen, Processing and

- characterization of ZrO_2 and Y-doped ZrO_2 powders, *Amer. Ceram. Soc. Bull.*, 64, 1985, 1115-1120.
18. B. Fegley Jr., E.A. Barringer, H.K. Bowen, Synthesis and Characterization of Monosized Doped TiO_2 Powders, *J. Amer. Ceram. Soc.*, 67, 1984, C113-C116.
19. V.Ya. Shevchenko, V.B. Glushkova, T.I. Panova, L.I. Podzorova, A.A. Il'icheva, A.E. Lapshin, Preparation of Ultrafine Tetragonal ZrO_2 - CeO_2 Solid Solutions, *inorganic materials* 37, 2001, 692-697.
20. V. Santos, M. Zeni, C.P. Bergmann, J. M. Hojemberger, Correlation between thermal treatment and tetragonal/monoclinic nanostructured zirconia powder obtained by sol-gel process, *Rev. Adv. Mater. Sci.*, 17, 2008, 62-70.
21. I. Georgieva, N. Danchova, S. Gutzov, N. Trendafilova, DFT modeling, UV-Vis and IR spectroscopic study of acetylaceton-modified zirconia sol-gel materials, *J. Mol. Model.*, 18, 2012, 2409-2412.